THE JOURNAL OF PHYSICAL CHEMISTRY A

Article

pubs.acs.org/JPCA

Resonance Raman Spectra and Electronic Transitions in Carotenoids: A Density Functional Theory Study

Mindaugas Macernis,*[,†,‡] Juozas Sulskus,[†] Svetlana Malickaja,[†] Bruno Robert,[§] and Leonas Valkunas[†,‡]

[†]Theoretical Physics Department, Faculty of Physics, Vilnius University, Saulėtekio al. 9, LT-10222 Vilnius, Lithuania

[‡]Center for Physical Sciences and Technology, A. Gostauto 11, LT-01108 Vilnius, Lithuania

[§]Institut de Biologie et de Technologie de Saclay, CEA, UMR 8221 CNRS, University Paris Sud, CEA Saclay, 91191 Gif sur Yvette, Paris, France

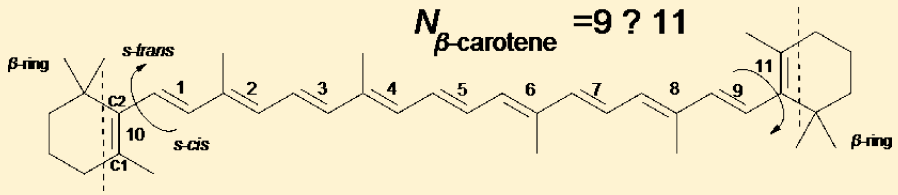

ABSTRACT: Raman and electronic absorption spectra corresponding to the S_0-S_2 electronic transition of various carotenoid and polyene molecules are theoretically analyzed using the density functional theory (DFT) approach. The results demonstrate the linear dependence between the frequency of the so-called ν_1 band corresponding to the C═C stretching modes in the Raman spectra and the S_0-S_2 electronic transition for molecules of different conjugation lengths. From these calculations the following relationship have been identified: (i) the effective conjugation length shortens in conformers of carotenoids containing β-rings whereas it increases in polyene upon *s-cis* isomerization at their ends, (ii) methyl groups connected to the conjugated chain of carotenoids induce a splitting of the ν_1 band in the Raman spectra, (iii) the effective conjugation lengths of *all-trans*-polyenes and corresponding *all-trans*-carotenoids are the same as follows from the Raman ν_1 frequency, but they are different as defined from S_0-S_2 electronic transition energies. The results well correlate with the experimental observations.

INTRODUCTION

Carotenoids (Cars) are organic molecules of the natural origin made of isoprenoid units (Figure 1A). They play a number of essential functions in photosynthesis such as harvesting the light in the blue-green region, where chlorophylls poorly absorb, and are involved in photoprotection of the photosynthetic apparatus.[1−4] They are also responsible for efficient quenching of the excited singlet and triplet states of chlorophyll molecules. The later process of the triplet quenching is directly related to Cars ability to stimulate the transition of the $^1O_2$ molecule to its ground state, which is the triplet state.[5,6] All these carotenoid functions tightly depend on the properties of their lowest electronic excited states.

Predicting the electronic structure of Car molecules is a complex task. Natural carotenoids may be purely linear with the cycle groups at the ends of the conjugated chain (e.g., β-carotene contains two such cycles; see Figure 1A), or with several functional groups, conjugated or not with the isoprenoid chain.[3] This is one of the reasons these molecules display an amazing variety of spectroscopic and functional properties, which are still poorly understood. The absorption spectrum of Cars depends on both the length of the conjugated chain and solvent properties.[7−12] Their absorption bands in the visible spectral range correspond to a S_0-S_2 electronic transition,[13] whereas a lower, S_1, state is absorption-silent, as was predicted in the 1970s.[14] In addition to this "dark" S_1 state, from the analysis of the time-resolved experiments, more low-energy excited states have been proposed to be also present in carotenoids.[5,15,16] A direct relationship between the S_0-S_2 absorption band and the length of the conjugated chain has been established many decades ago.[17−21]

Recently, using combination of resonance Raman and electronic absorption, new attempts were performed to explain Cars absorption in different environments, including proteins and tissues.[22] Resonance Raman, as a vibrational technique, is an ideal method to study structural properties of molecules, as it yields direct access to the molecular properties of their electronic ground state. Resonance Raman spectra of Cars contain three main bands indicated as ν_1, ν_2, ν_3, shown in the inset of Figure 2. The ν_1 band arises from the stretching modes of the C═C bonds. It thus gives access to the structure of the conjugated double bond chain; i.e., this frequency can be considered as a direct measure of the conjugation length of the chain.[23] As a conjugation length we assume here the number of C═C double bonds in the polyene chain. However, resonance Raman experiments showed that properties of even simple Car molecules in solvents had to be re-examined.[22] As a result of this study, as an example, the effective conjugation length of β-carotene was reassessed from 11 to 10 double bonds.

Received: June 30, 2013
Revised: February 4, 2014
Published: February 15, 2014

   dx.doi.org/10.1021/jp406449c | *J. Phys. Chem. A* 2014, 118, 1817−1825

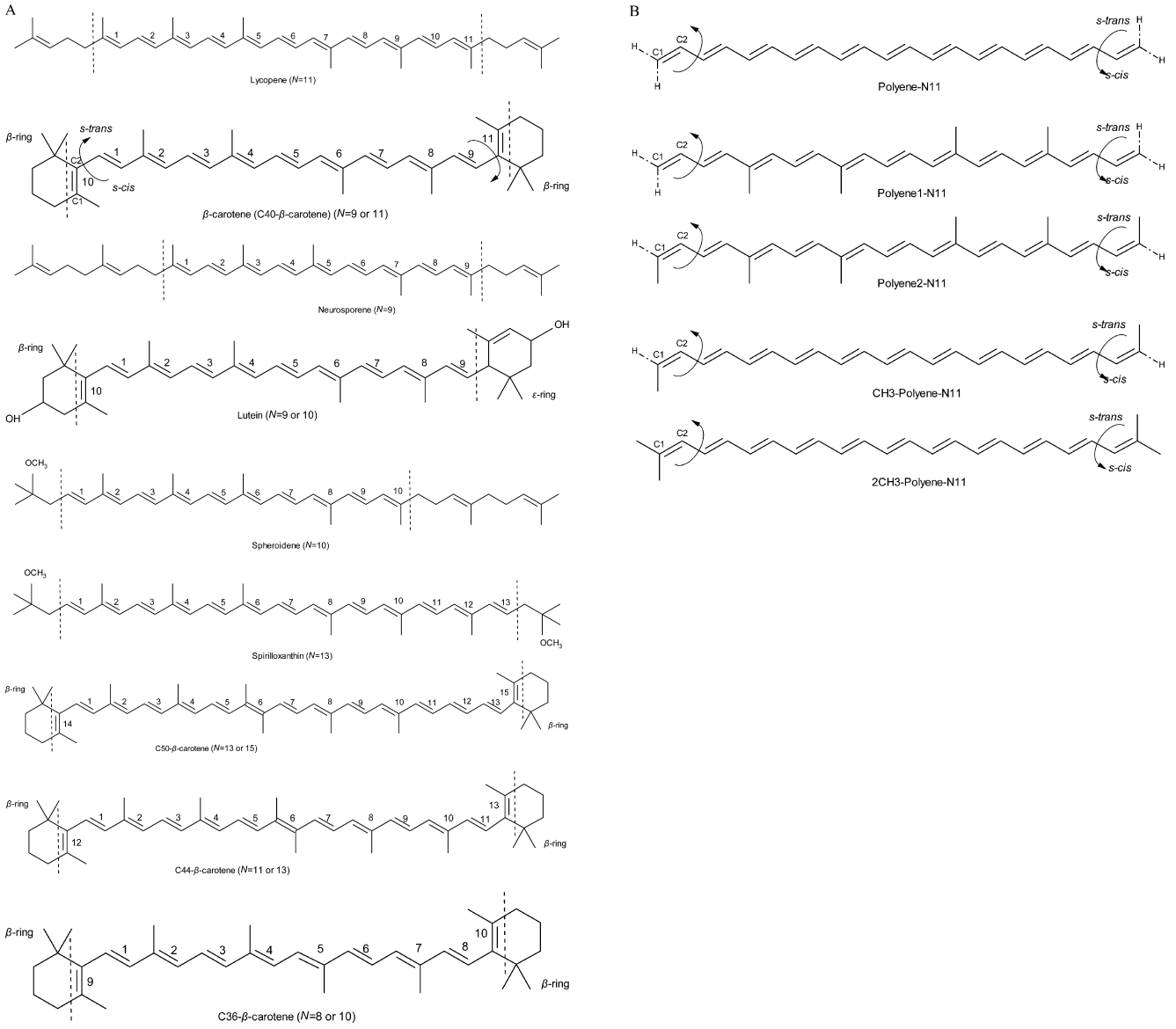

Figure 1. Molecular structures under consideration: (A) carotenoid molecules; (B) artificially made polyenes and β-carotene structures.

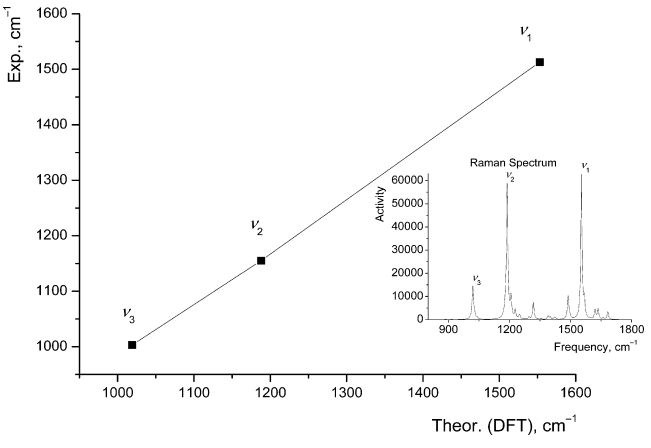

Figure 2. Correlation between calculated and experimental[22] Raman band positions (lycopene case). Inset: a typical calculated resonance Raman spectrum of a carotenoid molecule (lycopene case).

It is known that the effective conjugation length depends on the type and number of functional groups attached to the ends of conjugated system and carbon backbone.[24−26] Such conjugation length can be determined from the results of experimentally determined excited states lifetimes,[25−29] or absorption and Raman spectra of conjugated systems in solvents.[30,31] Dependencies of conjugation length on structural distortions of carotenoids were investigated by means of theoretical quantum chemistry methods.[30−34] However, the conjugation lengths properties of different molecule groups (Cars, Cars with β-ring, pure polyene, etc.) are not clear.

Effective conjugation length depending only on the fraction of double C═C bond for various Cars was introduced by using the linear dependence between Raman frequency and absorption band energy.[22] However, the basics of such a definition of the effective conjugation is not well-defined. For better understanding, comparative studies of Cars and pure polyenes by analyzing the sensitivity of the Raman spectrum and the S_0−S_2 transition energy to the effective conjugation length would be helpful in determining this type of definition. Therefore, here we will present such studies by investigating

dx.doi.org/10.1021/jp406449c | J. Phys. Chem. A 2014, 118, 1817−1825

various polyenes and Cars together with different artificial structures relevant to this issue.

Using quantum chemical calculations, we have modeled the Raman spectra and optical transitions of nine simple carotenoid molecules. Calculations performed on simpler polyene chains with different substitutions allow us to pinpoint the molecular origin of the carotenoid properties. This led us to address the influence the carotenoid functional groups on their Raman and optical absorption spectra. Finally, as it was recently shown that polarizability had a small but significant effect on the carotenoid ground state, we have also modeled the resonance Raman spectra and S_0-S_2 transitions of lutein in different solvents.

COMPUTATIONAL METHODS

Correlation between the absorption bands of polyenes and carotenoids and the frequencies of the ν_1 Raman band depending on their conjugation length have been experimentally identified.[22] As has been shown, the longer the conjugation length, the lower is energy of the S_0-S_2 transition and the lower is the ν_1 frequency. However, as underlined,[24] carotenoids possessing conjugated cycles do not strictly follow these relationships. Mendes-Pinto et al. proposed that distortion of the cycle conformation, leading to its partial deconjugation could be at the origin of this phenomenon.[22] These molecules thus differ from pure polyene chain by (i) their CH_3 groups conjugated with the polyene chain and (ii) their β-rings at the ends of the polyene chain, often in a *s-cis* conformation. To quantitatively analyze what happens with cyclic carotenoid molecules, computations of various polyenes and Car molecules in their both *s-cis* and *s-trans* conformations were carried out to compare with the results obtained for cyclic carotenoids.

For lycopene (*all-trans*-lycopene) and lutein, as starting geometry, we used the structures present in the protein data bank, 1LGH[35] and 1RWT,[36] respectively, to which we added the missing hydrogen atoms. Other Cars, displayed in Figure 1, were artificially constructed. Altogether, calculations were thus performed for lycopene, neurosporene, spheroidene, lutein, spirilloxanthin, and C50-β-carotene, C44-β-carotene, C40-β-carotene (β-carotene), and C36-β-carotene. The structures of the molecules are displayed in Figure 1A.

For analyzing precisely the influence of substituted methyl groups and end cycles on electronic properties, we performed calculations yielding geometry optimization with a subsequent calculations of the Raman spectra and the excitation energies corresponding to the transition to the optically allowed state $1^1B_u^+$ (S_0-S_2 transition) for two groups of molecules. The first one comprises pure polyene chains of different lengths, containing the conjugation length from $N = 8$ to $N = 13$. For all polyenes, calculations were performed on *all-trans* and 1-*s-cis* and 2-*s-cis* conformations, the latter assuming that one or both last C=C units of the polyene chain to be in the *s-cis* position. These typical *s-trans*, 1-*s-cis*, and 2-*s-cis* polyenes are shown in Figure 1B. The second group of molecules was designed to evaluate the role of the methyl substitutions and of the end cycles in carotenoid molecules. It comprises structures where these groups were progressively added to polyenes, to gradually confer to them β-carotene-like properties (Figure 1B).

The resonance Raman spectra were analyzed by attributing each Raman band to a particular vibrational mode of the molecule. Such attribution was performed in terms of quantum chemical calculations without taking into account the environmental influence on the spectrum. Thus, all calculations below are performed for Cars in a vacuum, except when indicated otherwise.

Calculations of the ν_1 Raman bands were performed for lycopene (linear polyene chain of length $N = 11$) and β-carotene (linear polyene chain of length $N = 9$ with a β-rings at each end) by the density functional theory (DFT) method using B3LYP/6-31G, B3LYP/TZVP, B3LYP/6-31G(2df,p), BP86/6-31G(d), BPW91/6-31G(d), B3P86/6-31G(d), B3PW91/6-31G(d), and SVWN/6-31G(d).[37] All methods based on the DFT are able to perform calculations of the vibrational frequency with overall root-mean-square errors (34−48 cm^{-1}), significantly less than that reported for the MP2 theory (61 cm^{-1}).[38] Comparison of the results obtained led to the conclusion that the B3LYP/6-31G(d) method is good enough to obtain reasonable results. A scaling factor 0.9613 was set for frequencies calculated by this method to obtain a satisfactory agreement with experimental data.[38]

Calculations were performed using three different basis sets: 6-31G(d), 6-311G(d,p), and cc-pVDZ, available in the Gaussian 09 package (Rev C.01).[39] The last two basis sets yield quite similar results by estimating lengths of the carbon−carbon bonds in the optimized geometry (Table 1). The hybrid B3LYP functional in combination with 6-311G(d,p) basis sets is known to provide reasonably good geometries.[40] The correlation between calculation data obtained by means of B3LYP/6-311G(d,p) and experimentally defined frequencies between 950 and 1600 cm^{-1} for lycopene[22] are presented in Figure 2 and Table 2. The predicted Raman intensity is largely concentrated in three spectral regions: around 1000 cm^{-1}, between 1100 and 1300 cm^{-1}, and between 1500 and 1550 cm^{-1}, which is in good correspondence with the experimental observations (Figure 2). Using the B3LYP/6-311G(d,p) method, a scaling factor about 0.9 has to be utilized (Table 2).[38]

Table 1. C−C Bond Lengths (R_{CC}, Å) of the Lycopene Calculated in the Optimized Geometry Using the B3LYP Functional

R_{bond}[a]	6-31G(d)	6-311G(d,p)	cc-pVDZ
1	1.355	1.352	1.349
1−2	1.445	1.444	1.441
2	1.36	1.357	1.354
2−3	1.448	1.446	1.443
3	1.371	1.368	1.365
3−4	1.433	1.431	1.428
4	1.366	1.363	1.36
4−5	1.442	1.440	1.437
5	1.375	1.372	1.369
5−6	1.428	1.426	1.423
6	1.369	1.366	1.363
6−7	1.428	1.426	1.423
7	1.375	1.372	1.369
7−8	1.442	1.440	1.437
8	1.366	1.363	1.36
8−9	1.433	1.431	1.428
9	1.371	1.368	1.365
9−10	1.448	1.446	1.443
10	1.36	1.357	1.354
10−11	1.445	1.444	1.441
11	1.355	1.352	1.349

[a]Figure 1A, lycopene.

dx.doi.org/10.1021/jp406449c | J. Phys. Chem. A 2014, 118, 1817−1825

Table 2. Calculated Frequencies and Relative Resonance Raman Intensities of the Lycopene Using Different Basis Sets

	ν_1		ν_2		ν_3	
data	freq, cm^{-1}	int, %	freq, cm^{-1}	int, %	freq, cm^{-1}	int, %
6-31G(d)	1573	46	1204	45	1034	9
6-31G(d)[a]	1512		1157		994	
6-311G(d,p)	1553	45	1188	45	1019	10
cc-pVDZ	1554	45	1192	45	1013	10
exp[22]	1513	37	1155	40	1003	23

[a]With scaling factor 0.9613 from ref 38.

The lowest electronic excited states are mainly defined by the excited states of the polyene chain. The transition from the ground state to the first excited state ($2^1A_g^-$) is forbidden due to the symmetry restrictions,[14,41,42] and it has a double excitation character ($HOMO^2 \rightarrow LUMO^2$). The optically allowed transition into the second excited state of the $1^1B_u^+$ symmetry is mainly caused by the HOMO → LUMO transition. It is known that the excited state of the $1^1B_u^+$ symmetry (corresponding to the S_0-S_2 transition) for the polyenes and Cars can be predicted in terms of the TD-DFT theory.[40,41] The energy value for β-carotene corresponding to the first optically allowed transition in the gas phase was reported to be between 2.85 and 2.93 eV.[43] This value is 0.62 eV higher than the excitation energy calculated using TD-DFT at the B3LYP/6-311G(d,p) level. The geometry parameters of all structures were optimized using the B3LYP/6-311G(d,p) method. The same level of the DFT calculations was used for both estimating the ν_1 Raman activity and evaluating the S_0-S_2 excitation energies. So, the DFT and TD-DFT methods using B3LYP/6-311G(d,p) calculation level were used in this work. When the solvent influence was considered, the polarizable continuum model (PCM) implemented in the Gaussian 09 package was used by choosing default parameters.

RESULTS

Calculations of Raman and optical absorption spectra for the ensemble of polyene molecules yield the linear correlation between the S_0-S_2 transition energies and the ν_1 Raman band positions (Figure 3). According to our results, the *s-cis* conformations of the polyenes containing the end groups result an increase of the π-conjugation length. The S_0-S_2 transition energy for the *s-trans* structure is 0.017 eV higher compared with the energy for the 2-*s-cis* structure with $N = 11$. If *all-trans*-polyene possesses a N conjugation length, its *s-cis* conformers will exhibit a ν_1 Raman frequency and a S_0-S_2 transition energy corresponding to those of a polyene with a conjugation length between N and $N + 1$. The *all-trans*-polyenes generally exhibit the lowest ground-state energies for any N.

However, this is not the case when the *s-cis* conformation occurs at the level of the β-ring in β-carotene (Figure 3, inset). In that case each β-ring formally adds one C=C bond to the conjugated polyene chain. For this molecule, calculations demonstrate the opposite effect. Upon *s-cis* isomerization, the ν_1 Raman frequency upshifts and gets a frequency corresponding to a π-conjugation length between $N - 1$ and N (Figure 3, inset). Formally, β-carotene should exhibit a conjugation length equivalent to that of polyene with $N = 11$. The presence of two β-rings in *s-cis* geometry makes it similar to 2-*s-cis*-β-carotene.

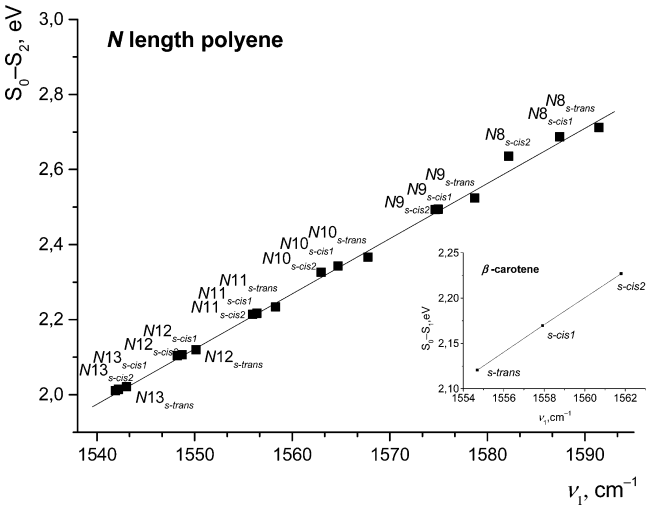

Figure 3. Correlation between the ν_1 Raman band position and the S_0-S_2 electronic transition energies calculated for polyenes with different lengths (N) of a conjugated polyene chain.

The ground-state energy of β-carotene is by 0.1165 eV lower than that of *all-trans*-β-carotene and by 0.0517 eV lower than that of 1-*s-cis*-β-carotene. When the calculated zero point vibrational energy is taken into account, the total energy of β-carotene becomes even lower, by 0.14 eV in comparison with the energy for *all-trans*-β-carotene and by 0.05 eV in comparison with the energy for 1-*s-cis*-β-carotene. The influence of *s-cis* isomerization on the position of electronic transitions of β-carotene is thus opposite to that obtained for pure polyene chains. As well, the presence of 2-*s-cis* conformation upshifts the position of the ν_1 Raman band of β-carotene by 7.108 cm^{-1} as compared to the position in the *all-trans* structure, whereas in the $N = 11$ polymer, the same conformation downshifts this band by 1.896 cm^{-1} (Table 3).

The CH_3 groups and β-rings are the main structural differences between β-carotene and *all-trans*-polyenes. To understand the influence of these structural changes on the

Table 3. Calculated S_0-S_2 Excitation Energies, ν_1 Raman Band Positions of the Polyene Chain in Artificially Made Structures of the β-Carotene

structure	E, eV	ν_1, cm^{-1}	ν_{1split}, cm^{-1}
s-trans-polyene-N11	**2.2338**	**1558.3202**	
1-*s-cis*-polyene-N11	2.2231	1556.9687	
2-*s-cis*-polyene-N11	2.2168	1556.4246	
s-trans-β-carotene	2.1204	1554.6933	1568.2095
1-*s-cis*-β-carotene	2.1696	1557.9232	1569.6547
β-carotene (2-*s-cis*-β-carotene)	**2.2271**	**1561.8013**	**1571.2836**
s-trans-polyene1-N11	**2.2102**	**1555.8697**	**1569.0444**
1-*s-cis*-polyene1-N11	2.2059	1555.2511	1569.1049
2-*s-cis*-polyene1-N11	2.2027	1554.7217	1569.2723
s-trans-polyene2-N11	2.1728	1554.4646	1568.3410
1-*s-cis*-polyene2-N11	2.1885	1555.4814	1569.0047
2-*s-cis*-polyene2-N11	**2.2051**	**1556.7979**	**1570.0326**
s-trans-CH3-polyene-N11	2.1944	1556.4863	
1-*s-cis*-CH3-polyene-N11	2.2109	1558.9427	
2-*s-cis*-CH3-polyene-N11	**2.2202**	**1558.8814**	
s-trans-2CH3-polyene-N11	2.1559	1554.5806	
1-*s-cis*-2CH3-polyene-N11	2.1763	1557.5660	
2-*s-cis*-2CH3-polyene-N11	**2.1924**	**1558.2487**	

dx.doi.org/10.1021/jp406449c | J. Phys. Chem. A 2014, 118, 1817−1825

S_0-S_2 transition energy and the ν_1 Raman band positions, model structures intermediate between N = 11 polyene and β-carotene were artificially constructed. Starting from pure *all-trans*-polyene, polyene1-N11 contains the methyl groups of β-carotene on its π-conjugated chain, and polyene2-N11 is constructed from polyene1-N11 but contains methyl groups at the ends of its π-conjugated chain. The specific influence of the latter group was studied by analyzing additional structures, CH3-polyene-N11, and 2CH3-polyene-N11, which do not contain the methyl groups conjugated with the π-conjugated chain, but only one or two methyl groups at the π-conjugated chain end, respectively (Figure 1B). For all these structures, *all-trans*, 1-*s-cis*, and 2-*s-cis* conformations were analyzed. The S_0-S_2 transition energies and ν_1 frequencies for all *s-trans*, 1-*s-cis*, and 2-*s-cis* conformers of these model structures are shown in Table 3.

The result of the calculations on these substituted polymers is quite clear. The main difference lies in the presence/absence of CH_3 groups at the end of the polyene chain. When methyl groups are present there, the lowest S_0-S_2 transition energies are obtained for 2-*s-cis* structures, whereas in structures where these methyl groups are absent, the lowest S_0-S_2 transition energies are obtained for *s-trans* structures. In the presence of methyl groups at the chain end, the *s-cis* conformation upshifts the ν_1 Raman frequency, whereas in the absence of these groups, the *s-cis* conformation downshifts the frequency of this mode (Table 3).

To explain achieved results from the electronic structures the additional analysis of Mulliken, electrostatic atomic charges (ESP) and HOMO−LUMO orbitals were performed. In the structures containing CH_3 groups connected to the polyene backbone (Figure 1B: polyene1-N11, polyene2-N11) the alternation of atomic charges on the carbon atoms in the polyene chain is much greater, and S_0-S_2 transition energies are smaller than in pure polyene chains (polyene-N11). It follows that the polyene1-N11 (and Cars) effective conjugation length determined from absorption spectra should be longer than in polyene-N11 (Figure 1A). Nevertheless, for further studies of the possible effect of the ending groups on the Cars spectra (Figures 3 and 4) we assume the conjugation length of the polyene chain in Cars and pure polyenes to be equal to the number of double C═C bonds. When β-rings or CH_3 groups are connected at the ends of the π-conjugated chain, the alternation of atomic charges on C1 and C2 atoms (Figure 1) increases and S_0-S_2 transition energies tend to the smaller values. Nevertheless, the transition energy differences are sometimes smaller than 0.01 eV, and this accuracy is not enough for strict conclusion. The analysis of π type HOMOs and LUMOs of corresponding *s-cis* structures show that contribution of atomic orbitals from C1 and C2 atoms to molecular orbitals is smaller compared to that achieved for *s-trans*. For pure polyene chains the results are opposite. A similar result was achieved for β-carotene by means of the DFT B3LYP/6-31G(d) calculations by considering the β-ring rotation.[32] For *s-cis* structures it is known that the interaction of ending groups with the polyene chain leads to steric deformations.[26,32] The dihedral angles between the C1═C2 bond and the plane of the polyene chain of our optimized structures are about 21° for 2-*s-cis*-polyene-N11, 30° for the structures 2-*s-cis*-polyene2-N11, 2-*s-cis*-2CH3-polyene2-N11, and 50° for β-carotene. This deformation at the ends of polyene chains together with the influence of ending CH_3 groups or β-rings in Cars causes smaller participation of π orbitals from C1 and C2 atoms in HOMO and LUMO of the polyene chain and it results in diminishing of the effective conjugation lengths.

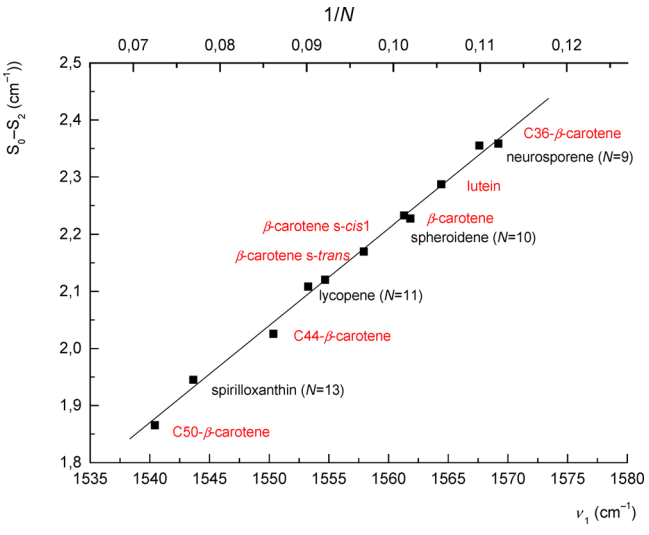

Figure 4. Correlation between the S_0-S_2 electronic transition energy and the ν_1 Raman band position calculated for Cars under consideration.

Additionally, we may compare the influence of the presence of the conjugated methyl groups on the nature of the vibrational modes, by comparing the N = 11 polyene with polyene1-N11 and polyene2-N11, which differ only by the presence of CH_3 groups bound to the π conjugated chain. In pure polyene, the ν_1 frequency arises from the asymmetric stretching vibration of the ═C—C═C− bond mixed with a bending vibration of the C—C—H valence angles. The presence of the CH_3 groups to the conjugated chain results in partitioning of the carbon atoms of the chain into two subsets of carbon atoms, those connected with H atoms, and those connected with CH_3 groups. The ν_1 mode splits accordingly into two asymmetric, mainly −C—C═C− stretching vibrations. The one mainly arising from the subset of carbon atoms connected with CH_3 displays a lower frequency whereas that mainly arising from the subset of carbon atoms connected with H atoms displays a slightly higher frequency (ν_1 and ν_{1split}, respectively; Table 3). For both modes, the largest nuclear motions occur close to the center of the polyene chain. This splitting is observed in all *s-trans*, 1-*s-cis*, and 2-*s-cis* conformations, and it is the largest (14.551 cm^{-1}) for 2-*s-cis*-polyene1-CH_3−N11, and the lowest splitting (9.482 cm^{-1}) for β-carotene (Table 3). In experimental Raman spectra, the ν_1 band is broad, and the ν_1 and ν_{1split} frequencies cannot be clearly distinguished. Moreover, calculations show that the Raman intensity of the ν_{1split} is much weaker than that of ν_1.

Calculations performed on different carotenoid molecules reflect exactly what was obtained for the differently substituted polymers. A strict linear dependence between the position of the S_0-S_2 transition and the frequency of the ν_1 Raman band is obtained, as expected for all carotenoid molecules studied (Figure 4). However, for neurosporene, spheroidene, lycopene, and spirilloxanthin, which do not possess cycles at the end of the π-conjugated chain, the conjugation length corresponds to that expected from the chemical structure, i.e., 9, 10, 11, and 13, respectively. In contrast, for all molecules possessing β-rings at

dx.doi.org/10.1021/jp406449c | J. Phys. Chem. A 2014, 118, 1817−1825

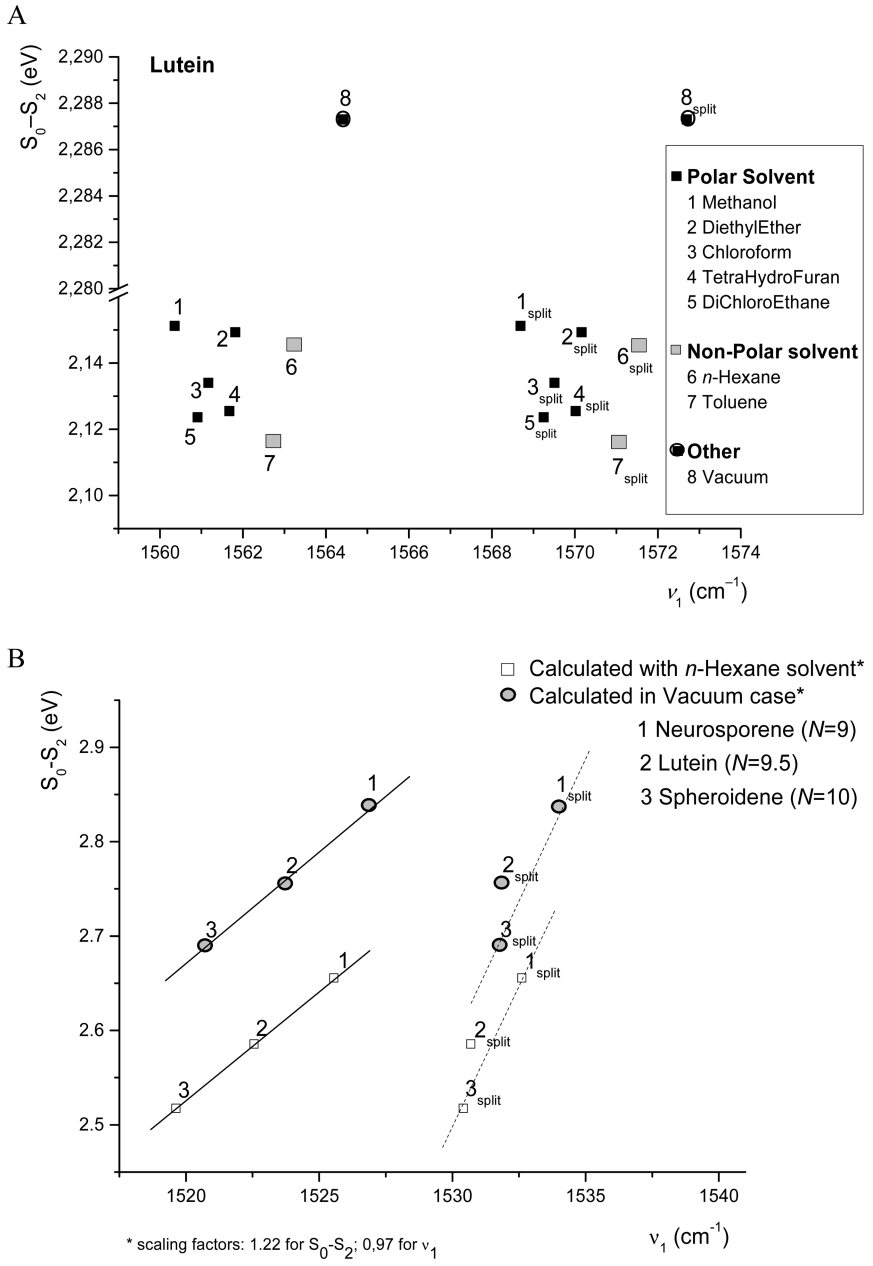

Figure 5. Correlation between the S_0−S_2 electronic transition energy and the ν_1 Raman band position: (A) calculation results for lutein in different solvents (the computed values presented without the scaling factor); (B) calculations in a vacuum and in *n*-hexane solvent (taking into account the scaling factor 1.22 for S_0−S_2 transition energies and 0.97 for the ν_1 values).

each end of the chain, namely, C50-β-carotene, C44-β-carotene, and C36-β-carotene, as well as for the lutein which contains only one single conjugated β-ring at one end, a shortening of the conjugation length is observed. These results allow us to estimate the influence of the β-rings on the extent of the π-conjugated chain. The S_0−S_2 transition energy for β-carotene and spheroidene are similar, and equal to 2.23 eV. This means that the effective conjugation length of β-carotene should be close to that of spheroidene, i.e., 10. Similarly, lutein (which contains a single β-ring) corresponds to a carotenoid with a conjugated length N of 9.5 in a vacuum (Figure 4).

Finally, we performed calculations designed to characterize the influence of solvents on the properties of the carotenoid molecules using PCM. Calculations were first achieved on lutein in different solvents, namely, methanol, diethyl ether, chloroform, tetrahydrofuran, dichloroethane, *n*-hexane, and toluene, solvents for which we had access to Raman experimental data[22] (Figure 5A). The splitting of the ν_1 Raman band of lutein, observed in a vacuum, is also present in all solvents, with a value of about 8.3 cm^{-1} in all cases. We observe a small, but clear, effect of the solvent polarizability on the carotenoid ground state. Indeed, while the S_0−S_2 transition energy corresponding to the π-electron excitation decreases according to solvent polarizability (as expected), the values of both ν_1 and ν_{1split} frequencies also decrease as compared to the value in a vacuum, and this is also in accord with the solvent polarizability (Figure 5). We actually observe that the strength of valence bonds changes in the presence of the solvents, thus modulating the π-electronic system in the π-conjugated chain.

dx.doi.org/10.1021/jp406449c | J. Phys. Chem. A 2014, 118, 1817−1825

The same phenomenon of ν_1 and ν_{1split} observed for the neurosporene, lutein, and spheroidene, the three carotenoid molecules for which we conducted calculations in hexane (Figure 5B). Describing the influence of the solvent, we find that the effective conjugation length as defined from the relation between the ν_1 Raman frequency and the S_0-S_2 transition energy shift gets smaller. As observed in a vacuum, the values obtained for lutein in hexane lead to the conclusion that the conjugation length of this carotenoid should be midway between that of neurosporene (N = 9) and spheroidene (N = 10), i.e., again N = 9.5, in remarkable agreement with published experimental data.[22] It is worth noting here that we observe an additional phenomenon concerning the ν_{1split} of lutein. Indeed, the ν_{1split} frequency in spheroidene is almost the same as that in lutein (Figure 5B). The analysis of vibrational forms shows that the ν_{1split} vibration in lutein corresponds to the vibration of the C═C valence bond from the β-ring, which vibrates together with all the chain. So the ν_{1split} vibration in lutein and spheroidene is actually the vibration of the polyene with N = 10 and the frequency in both Cars is almost the same.

DISCUSSION

In this paper, using theoretical modeling by DFT methods, we performed a complete analysis of the resonance Raman spectrum of lycopene. The calculated frequency values, however, differ from the experimental data depending on the computational level; thus, to fit with experimental data, a scaling factor is required.[39] Calculations of lycopene unequivocally show that the combination of the 6-31G(d,p) basis set and the B3LYP exchange−correlation functional provides an accurate description of the vibrational modes for a molecule of this size. It yields attributions of the main resonance Raman bands similar to previously published results.[39] The ν_1 (1553 cm^{-1}) vibrational mode mainly reflects the stretching vibrations of the C═C bonds. The ν_2 (1188 cm^{-1}) vibrational mode arises from linear combinations of the stretching of the C—C bonds and vibrations of the in-plane C—C—H valence angles of the polyene chain except for those parts of the conjugated chain that carry methyl groups. The ν_3 (1019 cm^{-1}) vibrational mode arises from linear combinations of the stretching of all C—C bonds and in-plane C—C—H valence angle vibrations together with valence angle vibrations in the methyl groups.

Here we applied the DFT to calculate the resonance Raman spectrum in the ground state and the energy of the S_0-S_2 transitions for different Cars. For linear carotenoids (spirilloxanthin, lycopene, spheroidene and neurosporene), we obtain, as expected, a near-to-perfect correlation between the inverse of their conjugation chain length N and the energies of their S_0-S_2 transitions, as well as with the frequency of their ν_1 Raman band (Figure 4). As experimentally observed,[44] Cars containing the cyclic end groups such as β-carotene, β-carotene derivatives and lutein clearly deviate from this correlation. However, even for these cyclic carotenoid molecules, an excellent correlation between the frequency of the ν_1 band and the energy of their S_0-S_2 transitions is observed. We may thus conclude that the electronic properties of β-carotene and cyclic carotenoid molecules may be described by taking into account the structure of their electronic ground state, which generally exhibit shorter effective conjugation length N. The C═C double bond from the β-ring extends the conjugation by only a fraction of a bond. This smaller contribution may be explained by the *s-cis* conformation of the C═C double bond of the ring. Using a series of substituted polyenes, we show that the presence of the CH_3 groups attached to the carotenoid conjugated chain induce a splitting of the ν_1 Raman band in all studied molecules. However, the analysis of π type HOMO and LUMO show that the presence of a C═C bond at the end of the π-conjugated chain of these structures induces a decrease of the contribution of atomic orbitals from end carbon atoms to molecular orbitals, thus resulting in shortening of the effective conjugated chain in *s-cis* conformation. Cars with β-rings connected to the polyene chain in the *s-cis* position thus exhibit effective conjugation lengths shorter than those for the polyene chain with a conjugated chain of the same length.

Shortening of the conjugated chain may also be induced by steric hindrance between the methyl group at the β-ring and the hydrogen atoms of the chain, which inhibits the required coplanarity of the ring with the chain, thus restricting its full conjugation, even in the *all-trans* configuration. We observe that the β-rings of β-carotene and lutein tend to adopt an out-of-plane twisted conformation, leading to a reduction of the conjugation of their C═C double bond with the rest of the isoprenoid chain of these molecules.

Much experimental and theoretical attention has been paid to the variations of the S_0-S_2 transitions of Cars caused by the environmental changes. The dependence of the position of the absorption transition of Cars according to the properties of the solvent has been extensively studied.[7,8,10−12,20,24] To the first approximation, it primarily depends on the refractive index of the considered solvent.[7,8,12] However, there is a current controversy on the respective roles of the refractive index and permittivity of the solvents in promoting the observed absorption shifts.[10,12] Dispersive solvent shifts occur when the states involved exhibit different stabilization energies. For Cars, the role of the different parameters of the environment leading to absorption shifts are still largely unknown, although dispersive forces were recently concluded to be the major factor driving the transition energy change, the red shifts caused by polarity being 1 order of magnitude smaller.[12] We show that the solvent polarizability induces a change of the molecule ground-state structure, resulting in a small but significant change in bond alternation, and accordingly, to a slight shift of the position of the ν_1 Raman mode, in excellent agreement with recently published data.[22] The apparent conjugation length of carotenoid molecules slightly extends when polarizability of the solvent increases, reflecting the response of the ground-state electronic structure to the properties of the solvent. A small but significant dependence of the position of this Raman mode is observed according to the energy of the S_0-S_2 transition, representing the effect of the solvent polarizability in the carotenoid ground state. The fact that it is small indicates that, as expected, polarizability affects both the structure of the ground and excited electronic states of the carotenoid molecule, and that these combined (actually entangled) effects result in the polarizability-induced absorption shift of the molecule.

CONCLUSIONS

Altogether, this study provides the theoretical framework to explain why and how resonance Raman spectroscopy can discriminate between the different effects underlying the small red shifts of the S_0-S_2 transition of carotenoid molecules. In particular, polarizability effects and changes in the effective conjugation length of these molecules can be distinguished due to the different correlation between the frequency of the ν_1 Raman band and the carotenoid absorption position. This

dx.doi.org/10.1021/jp406449c | J. Phys. Chem. A 2014, 118, 1817−1825

should be helpful in disentangling the different mechanisms underlying the red shifts of the S_0-S_2 observed in complex media, and in particular in proteins and in vivo.

The hybrid B3LYP functional in combination with 6-311G(d,p) basis sets provides reasonably good geometries of the molecules under consideration, and by determining the Raman spectra and the S_0-S_2 transition energies of pure polyene chains and Cars. The correlation is almost linear between the S_0-S_2 transition energies and the ν_1 Raman band positions for polyenes with the conjugation lengths from $N = 8$ to 13 and for carotenoids. Cars with β-rings connected to the ends of the polyene chain in the *s-cis* position are similar to *all-trans*-polyene of $N - 1$ effective conjugation length. CH_3 groups attached to the polyene chain backbone are responsible for splitting of the ν_1 Raman band in Cars and in polyene chains. As follows from calculated S_0-S_2 transition energies for such systems, the effective conjugation length increases in comparison with that of pure polyenes of the same length.

The Raman v_1 band and S_0-S_2 excitation have additional information about the β-ring position according to the polyene chain (Figure 4): the *s-trans* and *s-cis* conformations differ by half of the effective conjugation unit, which can be determined from the position of the S_0-S_2 excitation energy and the ν_1 band point in Figure 4 type diagrams. Moreover, on the background of theoretical modeling we can conclude that the polar solvent differently effects the Raman ν_1 band splitting causing different "effective conjugation lengths" for different ν_1 sub-band.

There are many examples of extreme shifts of the carotenoid absorption reported in biological systems, which generally determine the function of these molecules. Our present calculations mainly concern limited (0.2 eV) carotenoid absorption shifts. However, we are currently extending our approach to situations where larger absorption shifts are observed.

AUTHOR INFORMATION

Notes

The authors declare no competing financial interest.

ACKNOWLEDGMENTS

The public access supercomputer from the High Performance Computing Center (HPCC) of the Lithuanian National Center of Physical and Technology Sciences (NCPTS) at Physics Faculty of Vilnius University was used. The study was partly funded from the Social Foundation of the European Community under Grant Agreement No. VP1-3.1-ŠMM-08-K-01-004/KS-120000-1756 (J.S. and S.M.) and by the Lithuanian-Latvian-Taiwan project TAP-LLT-12-003 (M.M. and L.V.). It was also financially supported by EU program Marie Curie (FP7 Initial Training Network HARVEST), by the ERC funding agency (PHOTPROT project), by the CEA interdisciplinary program Technology for Health (MEDIA-SPEC project), and by the National Research Agency (ANR, Cyanoprotect Project) (B.R).

REFERENCES

(1) Pascal, A. A.; Liu, Z. F.; Broess, K.; van Oort, B.; van Amerongen, H.; Wang, C.; Horton, P.; Robert, B.; Chang, W. R.; Ruban, A. Molecular Basis of Photoprotection and Control of Photosynthetic Light-Harvesting. *Nature* **2005**, *436*, 134−137.

(2) Ruban, A. V.; Berera, R.; Ilioaia, C.; van Stokkum, I. H. M.; Kennis, J. T. M.; Pascal, A. A.; van Amerongen, H.; Robert, B.; Horton, P.; van Grondelle, R. Identification of a Mechanism of Photoprotective Energy Dissipation in Higher Plants. *Nature* **2007**, *450*, 575−U22.

(3) *Carotenoids, Vol. 4: Natural Functions*; Britton, G., Liaasen-Jensen, S., Pfander, H., Eds.; Birkauser: Basel, Boston, 2008.

(4) Holt, N. E.; Zigmantas, D.; Valkunas, L.; Li, X. P.; Niyogi, K. K.; Fleming, G. R. Carotenoid Cation Formation and The Regulation of Photosynthetic Light Harvesting. *Science* **2005**, *307*, 433−436.

(5) Polivka, T.; Sundstrom, V. Ultrafast Dynamics of Carotenoid Excited States — From Solution to Natural and Artificial Systems. *Chem. Rev.* **2004**, *104*, 2021−2071.

(6) Foote, C. S. Photosensitizatized Oxidation and Singlet Oxygen: Consequences in Biological Systems. In *Free Radicals and Biological Systems*; Pryor, W. A., Ed.; Academic Press: New York, 1976.

(7) Le Rosen, A. L.; Reid, E. D. An Investigation of Certain Solvent Effect in Absorption Spectra. *J. Chem. Phys.* **1952**, *20*, 233−236.

(8) Hirayama, K. Absorption Spectra and Chemical Structures. I. Conjugated polyenes and p-Polyphenyls. *J. Am. Chem. Soc.* **1955**, *77*, 373−379.

(9) Andersson, P. O.; Gillbro, T.; Ferguson, L.; Cogdell, R. J. Absorption Spectral Shifts of Carotenoids Related to Medium Polarizability. *Photochem. Photobiol.* **1991**, *54*, 353−360.

(10) Kuki, M.; Nagae, H.; Cogdell, R. J.; Shimada, K.; Koyama, Y. Solvent Effect on Spheroidene in Nonpolar and Polar Solutions and the Environment of Spheroidene in the Light-Harvesting Complexes of Rhodobacter-Sphaeroides 2.4.1 as Revealed by the Energy of the (1)a(G)(-)-]B-1(U)+ Absorption and the Frequencies of the Vibronically Coupled C═C Stretching Raman Lines in the (1)a(G)-(-) and 2(1)a(G)(-) States. *Photochem. Photobiol.* **1994**, *59*, 116−124.

(11) Chen, Z. G.; Lee, C.; Lenzer, T.; Oum, K. Solvent Effects on the S-0(1(1)Ag(-)) → S-2(1(1)B(U)(+)) Transition of Beta-Carotene, Echinenone, Canthaxanthin, and Astaxanthin in Supercritical CO2 And CF3H. *J. Phys. Chem. A* **2006**, *110*, 11291−11297.

(12) Renge, I.; Sild, E. Absorption Shifts in Carotenoids-Influence of Index of Refraction and Submolecular Electric Fields. *J. Photochem. Photobiol. A* **2011**, *218*, 156−161.

(13) Tavan, P.; Schulten, K. The Low-Lying Electronic Excitations in Long Polyenes: A PPP-MRD-CI Study. *J. Chem. Phys.* **1986**, *85*, 6602−6609.

(14) Polivka, T.; Sundstrom, V. Dark Excited States of Carotenoids: Consensus and Controversy. *Chem. Phys. Lett.* **2009**, *477*, 1−11.

(15) Papagiannakis, E.; Kennis, J. T. M.; van Stokkum, I. H. M.; Cogdell, R. J.; van Grondelle, R. An Alternative Carotenoid-to-Bacteriochlorophyll Energy Transfer Pathway in Photosynthetic Light Harvesting. *P. Natl. Acad. Sci. U. S. A.* **2002**, *99*, 6017−6022.

(16) Wang, P.; Nakamura, R.; Kanematsu, Y.; Koyama, Y.; Nagae, H.; Nishio, T.; Hashimoto, H.; Zhang, J. P. Low-Lying Singlet States of Carotenoids Having 8−13 Conjugated Double Bonds as Determined by Electronic Absorption Spectroscopy. *Chem. Phys. Lett.* **2005**, *410*, 108−114.

(17) Dale, J. Empirical Relationships of the Minor Bands in the Absorption Spectra of Polyenes. *Acta Chem. Scand.* **1954**, *8*, 1235−1256.

(18) Hemley, R.; Kohler, B. Electronic Structure of Polyenes Related to the Visual Chromophore. A Simple Model for The Observed Band Shapes. *Biophys. J.* **1977**, *20*, 377−382.

(19) Christensen, R. L.; Barney, E. A.; Broene, R. D.; Galinato, M. G. I.; Frank, H. A. Linear Polyenes: Models for The Spectroscopy and Photophysics of Carotenoids. *Arch. Biochem. Biophys.* **2004**, *430*, 30−36.

(20) Araki, G.; Murai, T. Molecular Structure and Absorption Spectra of Carotenoids. *Prog. Theor. Phys.* **1952**, *8*, 639−654.

(21) Suzuki, H.; Mizuhuashi, S. π-Electronic Structure and Absorption Spectra of Carotenoids. *J. Phys. Soc. Jpn.* **1964**, *19*, 724−738.

(22) Mendes-Pinto, M. M.; Sansiaume, E.; Hashimoto, H.; Pascal, A. A.; Gall, A.; Robert, B. Electronic Absorption and Ground State Structure of Carotenoid Molecules. *J Phys. Chem. B* **2013**, *117*, 10974−10986.

(23) Saito, S.; Tasumi, M. Normal-Coordinate Analysis of Retinal Isomers and Assignments of Raman and Infrared Bands. *J. Raman Spectrosc.* **1983**, *14*, 236−245.
(24) Frank, H. A.; Bautista, J. A.; Josue, J.; Pendon, Z.; Hiller, R. G.; Sharples, F. P.; Gosztola, D.; Wasielewski, M. R. Effect Of The Solvent Environment On The Spectroscopic Properties And Dynamics Of The Lowest Excited States Of Carotenoids. *J. Phys. Chem. B* **2000**, *104*, 4569−4577.
(25) Frank, H. A.; Josue, J. S.; Bautista, J. A.; van der Hoef, I.; Jansen, F. J.; Lugtenburg, J.; Wiederrecht, G.; Christensen, R. L. Spectroscopic And Photochemical Properties Of Open-Chain Carotenoids. *J. Phys. Chem. B* **2002**, *106*, 2083−2092.
(26) Mendes-Pinto, M. M.; LaFountain, A. M.; Stoddard, M. C.; Prum, R. O.; Frank, H. A.; Robert, B. Variation In Carotenoid−Protein Interaction In Bird Feathers Produces Novel Plumage Coloration. *J. R. Soc. Interface* **2012**, *9*, 3338−3350.
(27) Fuciman, M.; Chábera, P.; Župčanová, A.; Hříbek, P.; Arellano, J. B.; Vácha, F.; Pšenčík, J.; Polívka, T. Excited State Properties Of Aryl Carotenoids. *Phys. Chem. Chem. Phys.* **2010**, *12*, 3112−3120.
(28) Polivka, T.; Frank, H. A. Molecular Factors Controlling Photosynthetic Light Harvesting by Carotenoids. *Acc. Chem. Res.* **2010**, *43*, 1125−1134.
(29) Chatterjee, N.; Niedzwiedzki, D. M.; Kajikawa, T.; Hasegawa, S.; Katsumura, S.; Frank, H. A. Effect Of π-Electron Conjugation Length On The Solvent-Dependent S_1 Lifetime Of Peridinin. *Chem. Phys. Lett.* **2008**, *463*, 219−224.
(30) Focsan, A. L.; Bowman, M. K.; Molnár, P.; Deli, J.; Kispert, L. D. Carotenoid Radical Formation: Dependence On Conjugation Length. *J. Phys. Chem. B* **2011**, *115*, 9495−9506.
(31) Merlin, J. C. Resonance Raman Spectroscopy Of Carotenoids And Carotenoidcontaining Systems. *Pure Appl. Chem.* **1985**, *57*, 785−792.
(32) Liu, W. L.; Wang, Z. G.; Zheng, Z. R.; Li, A. H.; Su, W. H. Effect Of B-Ring Rotation On The Structures And Vibrational Spectra Of B-Carotene: Density Functional Theory Analysis. *J. Phys. Chem. A* **2008**, *112*, 10580−10585.
(33) Golibrzuch, K.; Ehlers, F.; Scholz, M.; Oswald, R.; Lenzer, T.; Oum, K.; Kimc, H.; Koo, S. Ultrafast Excited State Dynamics And Spectroscopy Of 13,130-Diphenyl-B-Carotene. *Phys. Chem. Chem. Phys.* **2011**, *13*, 6340−6351.
(34) Vivas, M. G.; Silva, D. L.; de Boni, L.; Zalesny, R.; Bartkowiak, W.; Mendonca, C. R. Two-Photon Absorption Spectra Of Carotenoids Compounds. *J. App. Phys.* **2011**, *109*, 103529−8.
(35) Koepke, J.; Hu, X.; Muenke, C.; Schulten, K.; Michel, H. The crystal structure of the light-harvesting complex II (B800−850) from Rhodospirillum molischianum. *Structure* **1996**, *4*, 581−597.
(36) Liu, Z. F.; Yan, H. C.; Wang, K. B.; Kuang, T. Y.; Zhang, J. P.; Gui, L. L.; An, X. M.; Chang, W. R. Crystal Structure of Spinach Major Light-Harvesting Complex at 2.72 Angstrom Resolution. *Nature* **2004**, *428*, 287−292.
(37) Liu, W. L.; Wang, Z. G.; Zheng, Z. R.; Jiang, L. L.; Yang, Y. Q.; Zhao, L. C.; Su, W. H. Density Functional Theoretical Analysis of the Molecular Structural Effects on Raman Spectra of beta-Carotene and Lycopene. *Chin. J. Chem.* **2012**, *30*, 2573−2580.
(38) Wong, M. W. Vibrational Frequency Prediction Using Density Functional Theory. *Chem. Phys. Lett.* **1996**, *256*, 391−399.
(39) Frisch, M. J.; Trucks, G. W.; et al. *Gaussian 09*, revision C.01; Gaussian Inc.: Wallingford, CT, 2011.
(40) Dreuw, A.; Harbach, P. H. P.; Mewes, J. M.; Wormit, M. Quantum Chemical Excited State Calculations on Pigment-Protein Complexes Require Thorough Geometry Re-optimization of Experimental Crystal Structures. *Theor. Chem. Acc.* **2010**, *125*, 419−426.
(41) Macernis, M.; Sulskus, J.; Duffy, C. D. P.; Ruban, A. V.; Valkunas, L. Electronic Spectra of Structurally Deformed Lutein. *J. Phys. Chem. A* **2012**, *116*, 9843−9853.
(42) Duffy, C. D. P.; Chmeliov, J.; Macernis, M.; Sulskus, J.; Valkunas, L.; Ruban, A. V. Modeling of Fluorescence Quenching by Lutein in the Plant Light-Harvesting Complex LHCII. *J. Phys. Chem. B* **2012**, Article ASAP.
(43) Liu, W. L.; Wang, D. M.; Zheng, Z. R.; Li, A. H.; Su, W. H. Solvent Effects on The S-0 -> S-2 Absorption Spectra of Beta-Carotene. *Chinese Phys. B* **2010**, *19*, 013102−6.
(44) Angerhofer, A.; Bornhauser, F.; Gall, A.; Cogdell, R. J. Optical and Optically Detected Magnetic-Resonance Investigation on Purple Photosynthetic Bacterial Antenna Complexes. *Chem. Phys.* **1995**, *194*, 259−274.